Journal of Fluorine Chemistry 141 (2012) 29–34

Contents lists available at SciVerse ScienceDirect

Journal of Fluorine Chemistry

journal homepage: www.elsevier.com/locate/fluor

Removal of fluoride ions from aqueous solutions using protonated cross-linked chitosan particles

Ruihua Huang [a,*], Bingchao Yang [b], Qian Liu [a], Kelian Ding [a]

[a] College of Science, Northwest A&F University, Yangling, Shaanxi 712100, China
[b] Xi'an Institute of Geology and Mineral Resource, Xi'an, Shaanxi 710054, China

ARTICLE INFO

Article history:
Received 7 February 2012
Received in revised form 26 May 2012
Accepted 29 May 2012
Available online 7 June 2012

Keywords:
Protonated cross-linked chitosan particles
Fluoride
Adsorption
Isotherm

ABSTRACT

Protonated cross-linked chitosan particles (PCP) were used to remove fluoride from aqueous solution. PCP were characterized using FTIR, XRD and SEM. Adsorption isotherms, the effects of adsorbent dosage, pH, contact time and co-existing anions on adsorption process, and the regeneration ability of PCP were investigated. The optimum pH value was achieved at 7. The equilibrium was attained in 40 min. The presence of co-existing anions weakened fluoride adsorption on PCP, especially the high valence anions such as sulfate. The equilibrium data fitted well with Langmuir and Freundlich isotherm models, and the maximum monolayer adsorption capacity was 8.10 mg g^{-1} at room temperature. 0.1 M HCl was identified as the best eluent. Electrostatic attraction was the main driving force for fluoride adsorption.

1. Introduction

Fluoride is an essential element, indispensable for production and maintenance of healthy bones and teeth. Nevertheless, fluoride concentrations in drinking water above 1.5 mg L^{-1} may be detrimental to human health, leading to dental or skeletal fluorosis which is a chronic disease manifested by mottling of teeth in mild cases, softening of bones and neurological damage in severe cases [1–4]. The World Health Organization has specified the tolerance limit of fluoride content of drinking water as 1.5 mg L^{-1} in drinking water [5].

With the development of industry, increasing amount of wastewater containing fluoride is being released from various engineering processes, such as semiconductor manufacturing, coal power plants, electroplating, rubber and fertilizer production, etc. It was necessary to reduce fluoride concentration based on the consideration of human health. At present, the removal of fluoride from drinking water was often realized by these methods including precipitation [6], ion exchange [7,8], reverse osmosis [9] and electrodialysis [10]. However, most of these methods have the shortcomings such as high operational and maintenance costs, secondary pollution (generation of toxic sludge, etc.) and complicated procedure involved in the treatment. Among various methods used for defluoridation of water, the adsorption process is widely used and offers satisfactory results and seems to be a more attractive method for the removal of fluoride in terms of cost, simplicity of design and operation [11,12].

Biosorption is a technique for water treatment utilizing abundantly available biomaterials. Various biosorbents have been developed for fluoride removal. Among various biosorbents, chitin and chitosan-derivatives have gained wide attention as effective biosorbents due to their low cost and high contents of amino and hydroxyl functional groups which show significant adsorption potential for the removal of various pollutants such as metal and dye, etc. Only a few reports are available about its capacity to remove fluoride. However, its broad application is limited due to its poor acid stability and difficulties of separation from solution after adsorption, etc. Hence, it needs to be modified into a stable form before effective use. In addition, the free $-NH_2$ groups in chitosan are prone to be protonated and become into $-NH_3^+$, which would show greater tendency to adsorb anions relative to free $-NH_2$ groups. At present, chitosan was mainly molded in beads for defluoridation [13–15]. In this study, attempt would be made to develop protonated cross-linked chitosan particles (PCP), which would be stable and can be regenerated. Here, chitosan was molded in membranes, membranes were cross-linked, and then protonated, the resultant membranes were ground to obtain particles of 200-mesh size. These particles can remove fluoride from aqueous solution due to big specific surface area and many positive charges. Besides, PCP would have good subsidence, and could be separated from solution rapidly after adsorption. So PCP were employed to remove fluoride from aqueous solution in this work. Batch experiments were conducted to evaluate adsorption capacity and to determine the regeneration feasibility of PCP.

---

* Corresponding author. Tel.: +86 029 87092226.
E-mail address: huangrh20022002@yahoo.com.cn (R. Huang).

0022-1139/$ – see front matter © 2012 Elsevier B.V. All rights reserved.
http://dx.doi.org/10.1016/j.jfluchem.2012.05.022

2. Experimental

2.1. Materials

Chitosan powder (deacetylation degree is 90%) was acquired from Sinopharm Group Chemical Reagent Limited Company (China). All reagents used in this study, including NaF, $NaNO_3$, Na_2SO_4, HCl, NaOH, $NaHCO_3$, acetic acid and glutaraldehyde, were of analytical grade.

2.2. Preparation of cross-linked and protonated chitosan

To prepare chitosan membranes, 3.6 g of chitosan powder was dissolved in 120 mL of 2 wt% acetic acid solution. The solution was dissolved completely, and de-bubbled after 1 h standing reaction. 10 mL homogeneous solution was coated in a petri dish with a diameter of 35 cm, and then dried at 60 °C. Subsequently, 0.1 M NaOH solution was poured on the surface of dry membranes, and thus these membranes were separated from the petri dish. The wet chitosan membranes were extensively washed with de-ionized water to remove any NaOH.

The membranes were cross-linked with 2.5 wt% glutaraldehyde solution and the ratio of glutaraldehyde to chitosan membranes was approximately 25 mL g^{-1} of dry membranes. Cross-linking reaction occurred for 23 h at 60 °C and then cross-linked films were washed with de-ionized water to remove residual glutaraldehyde, dried at 60 °C for 2 h.

The cross-linked membranes were protonated for 1.5 h in concentrated hydrochloric acid at room temperature in order to effectively utilize the amino groups of chitosan for fluoride adsorption. These films was washed with de-ionized water to neutral pH, dried at 60 °C and was ground to obtain particles of 200-mesh size, which was used for adsorption studies. The specific surface area was found to be 4.37 $m^2\,g^{-1}$. The cross-linked and protonated chitosan particles were stable and not dissolved in acid or alkali solutions. Besides, it shown a good settlement, and could be separated from solution rapidly.

2.3. Sorption experiments

Batch experiments were performed to investigate the adsorption capacity of fluoride using PCP. About 0.6 g of PCP was added into 50 mL of NaF solution with a desired pH value. The pH of the medium was adjusted with 0.1 M HCl or 0.1 M NaOH solution. The mixture was shaken at a speed of 200 rpm. Samples were taken at predetermined time intervals for the analysis of fluoride concentrations in the solutions until adsorption equilibrium was reached. The defluoridation capacity of PCP was studied at different conditions such as initial fluoride concentrations, contact time, pH of the medium, etc. and the effect of coexisting anions on fluoride removal was also investigated.

The adsorption experiment about the equilibrium isotherm was conducted with varied initial fluoride concentration from 11.8 to 59.0 mg L^{-1} at four different temperatures (viz., 20, 30, 40 and 50 °C). Besides, the rate of fluoride removal was studied at different time intervals that were as long as 100 min using different initial concentrations (viz., 11.8, 33.6 and 35.4 mg L^{-1}) at pH 7 and 20 °C.

2.4. Analysis

The fluoride concentration was measured using Shanghai Leici acidity meter with the fluoride ion selective electrode PF-1 (Leici, Shanghai). The pH measurements were done with the same instrument with pH electrode. FTIR spectra of chitosan samples were obtained using FTIR spectrometer (Avatar-360, Nicolet) to confirm the presence of functional groups. X-ray diffraction (XRD) profiles of virgin chitosan, cross-linked chitosan, as well as protonated cross-linked chitosan were applied to observe the crystal structure transformation of PCP during the modification process using an X-ray diffraction (Japan) with Cu anode, running at 40 kV and 40 mA. Diffraction measurements were conducted within the 2θ angle of 3–50°, at the scanning rate of 4°/min. The images of PCP before and after adsorption of fluoride were examined by scanning electron microscope (SEM) (JEOLJSM-6380LV).

2.5. Desorption study

After performing the equilibrium study with different initial fluoride concentration ranging from 11.8 to 59 mg L^{-1}, fluoride-adsorbed PCP were collected by filtration, and regenerated using 50 mL of 0.1 M NaOH, 0.1 M HCl and 0.1 M H_2SO_4 solutions, respectively. These solutions were stirred for 1 h at a stirring speed of 200 rpm. PCP were removed and rinsed with distilled water and then reused for a new adsorption toward different initial fluoride concentration.

3. Results and discussion

3.1. Characteristics of PCP

FTIR spectra is a useful tool to identify functional groups in a molecule, as each specific chemical bond often has a unique energy absorption band and can obtain structural and bond information [16]. Fig. 1 represents the FTIR spectra of PCP and fluoride-treated PCP. In Fig. 1a, a sharp peak at 1650 cm^{-1} is attributed to $-NH_2$ bending vibration in PCP. And a peak at 1516 cm^{-1} is also observed in PCP, confirming the presence of NH_3^+ groups. However, this peak at 1516 cm^{-1} in the fluoride-adsorbed PCP (Fig. 1b) almost disappears owing to the strong electrostatic attraction between positive charged $-NH_3^+$ and negatively charged fluoride ions.

XRD profiles of original chitosan, cross-linked chitosan, and protonated cross-linked chitosan are shown in Fig. 2. The peaks at $2\theta = 12°$ and 20° are the natural crystal peaks of chitosan expressed in Fig. 2a. After chitosan is cross-linked by glutaraldehyde, the natural crystal peak at $2\theta = 12°$ disappears, as shown in Fig. 2b. Besides, when protonated by hydrochloric acid, the peak $2\theta = 20°$ weakens obviously as shown in Fig. 2c. The results indicated that the action forces of hydrogen bonds among molecules reduced during the modified process, and the crystal structure of chitosan became much more disordered, making $-NH_3^+$ in PCP more accessible for adsorption.

SEM (scanning electron microscopy) is one of the most widely used surface diagnostic tools. Samples of PCP before and after adsorption of fluoride were coated under a vacuum with a thin layer of gold and then examined by SEM. The SEM micrographs of PCP are presented in (Fig. 3). The apparent difference is observed between the image of PCP before adsorption and the one of PCP

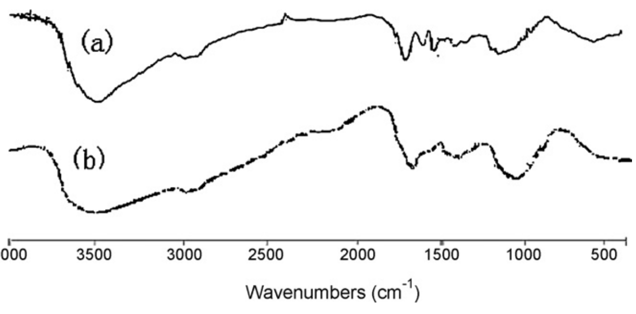

Fig. 1. FTIR spectra of (a) PCP and (b) PCP loaded by F^-.

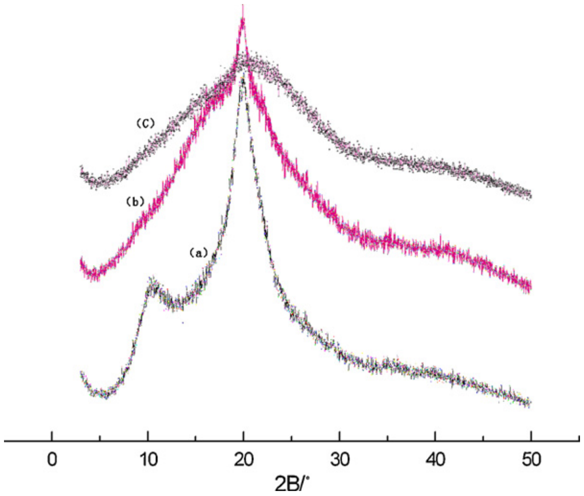

Fig. 2. XRD profiles of chitosan (a), cross-linked chitosan (b), and protonated cross-linked chitosan (c).

after adsorption. There is a loose distribution with many particles in PCP before adsorption, while PCP after adsorption becomes relatively compact. This difference indicated fluoride adsorption onto PCP.

3.2. Effect of adsorbent dosage

The adsorbent dosage is an important parameter for the determining of the adsorbability of adsorbent at a given initial condition. The influences of adsorbent dosage on fluoride adsorption are shown in Fig. 4. The fluoride removal increases with an increase in the dosage of PCP, which is obvious because of the increase in the number of active sites. When the dosage of PCP increases from 0.1 to 0.5 g, the fluoride removal increases from 53.5% to 83.9%. However, for the dosage of PCP more than 0.6 g, no significant increase in fluoride removal is observed. Hence, in all the subsequent experiments, 0.5 g of PCP was fixed as the optimum dosage which could give reasonably good removal toward fluoride.

3.3. Effect of contact time

Fig. 5 illustrates the removal of fluoride using PCP as a function of contact time in the range of 5–100 min at room temperature. The values are increasing sharply up to 40 min and thereafter it remains almost constant indicating the attainment of adsorption equilibrium. The nature of adsorbent and the available adsorption sites affect the rate of fluoride adsorption. The mechanism of solute transfer to the solid includes diffusion through the fluid film around the adsorbent particle and diffusion through the pores to the internal adsorption sites. In the initial stages of fluoride adsorption, the concentration gradient between the film and the available pore sites is large, and hence the rate of fluoride adsorption is faster. The rate of adsorption decreases in the later stages of fluoride adsorption is probably due to the slow pore diffusion of the solute ion into the bulk of the adsorbent. Therefore, 40 min of equilibrium time was chosen and this was used in all subsequent experiments.

3.4. Effect of pH

The solution pH is another important parameter. The variation of fluoride removals with pH is presented in Fig. 6. It is apparent that the maximum adsorption capacity is observed at pH 7. Decrease in adsorption capacities is observed below and above 7. Under acidic conditions, the amount of fluoride adsorbed is slightly decreased and this can be attributed to the formation of weak hydrofluoric acid. Under alkaline conditions, the decrease in fluoride removal may be due to the competition of excess hydroxyl ions with fluoride ions. Jagtap et al. [17] also show that the best performance of defluoridation of water using new modified chitosan-based adsorbent was obtained at neutral pH. For the following adsorption tests, pH of the solution was adjusted to 7.

3.5. Effect of initial fluoride concentration

Fig. 7 shows the variation of fluoride removals with respect to initial fluoride concentration at neutral pH and room temperature and the comparative difference between the cross-linked chitosan and PCP. Evidently, PCP have higher removal toward fluoride than the cross-linked chitosan. This clearly indicates that the protonated amine groups in PCP are responsible for higher removal than the original –NH_2 groups of chitosan. And it is observed that with an increase in initial fluoride concentration, the removal toward fluoride decreases, while the adsorption capacity increases. This may be because the amount of fluoride ions available for adsorption increases with the increase in concentration.

3.6. Effect of coexisting anions

Beside fluoride, the natural water always contains various other coexisting ions, which can compete for adsorption sites and result in the reduction in removal. To study the effect of coexisting anions, the fluoride removal using PCP is measured in the presence

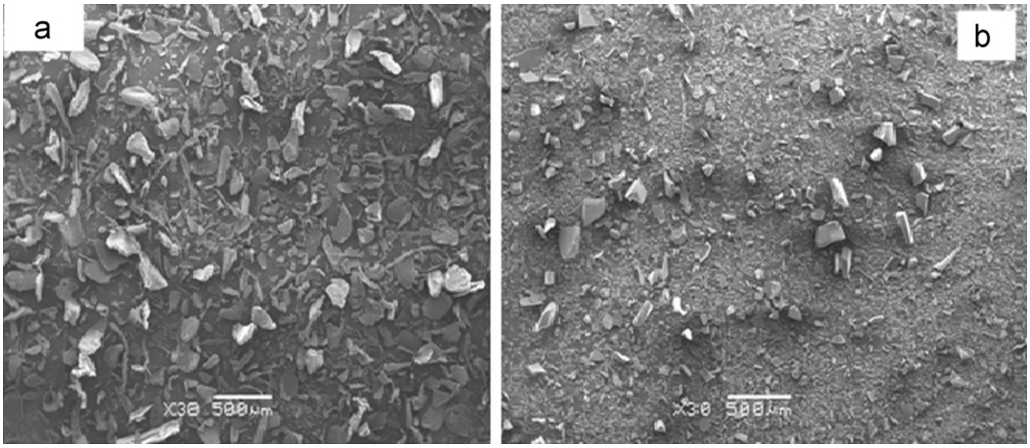

Fig. 3. SEM images of PCP before (a) and after (b) adsorbed by fluoride.

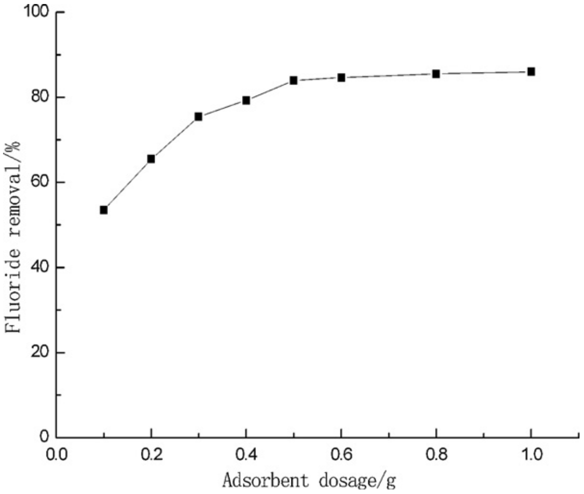

Fig. 4. Effect of adsorbent dosage on fluoride adsorption.

of various anions namely like HCO_3^-, Cl^-, NO_3^-, and SO_4^{2-} with the same concentration (400 mg L^{-1}) by keeping 11.8 mg L^{-1} and 23.6 mg L^{-1} as the initial fluoride concentration, respectively, at neutral pH and room temperature. The effect of coexisting ions on fluoride removal is shown in Fig. 8. It is observed that the presence of these ions weakens the fluoride adsorption on PCP, which results from the competition between fluoride and these ions such as sulfate, nitrate, and chloride for the sites on the adsorbent surfaces, especially for high valence anions such as sulfate. Besides, for HCO_3^-, a decrease in removal may be attributed to the increase in pH caused from the addition of HCO_3^-. As mentioned in Section 3.4, PCP showed a relatively low removal toward fluoride under alkaline conditions.

3.7. Equilibrium adsorption isotherm

Langmuir [18] and Freundlich [19] are the two commonly used isotherms to describe the adsorption characteristics of adsorbent. In the present investigation, the equilibrium adsorption data are analyzed according to the linear form of the Langmuir and Freundlich isotherm models. The linear form of Langmuir isotherm is given by Eq. (1):

$$\frac{C_e}{q_e} = \frac{1}{Qb} + \frac{C_e}{Q} \tag{1}$$

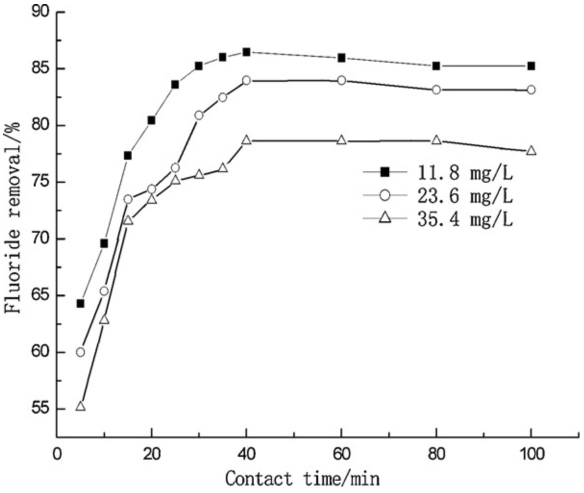

Fig. 5. Effect of contact time on fluoride adsorption.

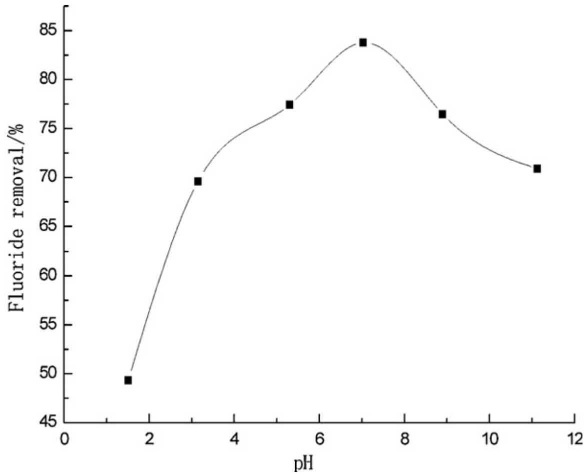

Fig. 6. Effect of pH on fluoride adsorption.

where C_e (mg L^{-1}) is the equilibrium fluoride concentration in solution, q_e (mg g^{-1}) is the amount of adsorption per unit mass of adsorbent at equilibrium (mg g^{-1}), b is adsorption equilibrium constant (L mg^{-1}) that is related to the apparent energy of adsorption and Q is the quantity of adsorbate required to form a single monolayer on unit mass of adsorbent (mg g^{-1}). The Langmuir isotherm constants Q and b are calculated from the slope and intercept of the plot C_e/q_e vs. C_e shown in Fig. 9 and the results are listed in Table 1. The values of Q are found to increase with rise in temperature, which indicates that the sorption capacity increases with rise in temperature. The high correlation coefficient (R^2) >0.97 indicates that fluoride adsorption onto PCP fits the Langmuir model. In other words, the adsorption of fluoride onto PCP is taken place at the functional groups/binding sites on the surface of PCP which is regarded as monolayer adsorption.

In order to find out the feasibility of the isotherm, the essential characteristics of the Langmuir isotherm can be expressed in terms of the dimensionless constant separation factor or equilibrium parameter [20],

$$R_L = \frac{1}{1 + bC_o} \tag{2}$$

where b is the Langmuir isotherm constant and C_o is the initial concentration of fluoride (mg L^{-1}). The R_L values at different

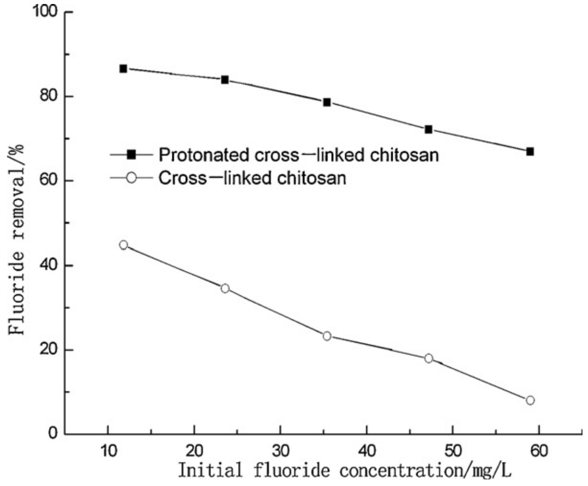

Fig. 7. Effect of initial fluoride concentration on fluoride adsorption.

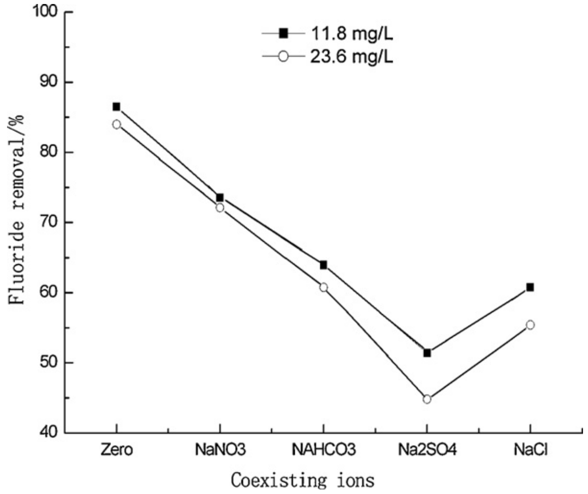

Fig. 8. Effect of coexisting ions on fluoride adsorption.

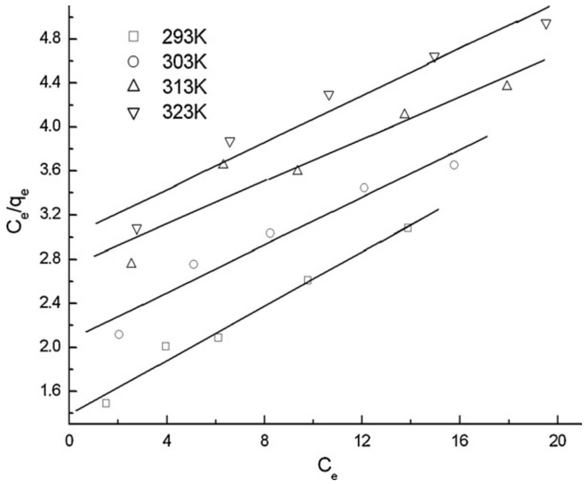

Fig. 9. Langmuir isotherm plots for fluoride adsorption on PCP.

temperatures studied are calculated and given in Table 1. The R_L values lying between 0 and 1 indicate the favorable conditions for adsorption at all the temperatures studied.

The linear form of Freundlich equation is given by Eq. (3)

$$\ln q_e = \ln K_f + \frac{1}{n} \ln C_e \quad (3)$$

where K_f (L g^{-1}) is the Freundlich adsorption isotherm constant relating to the extent of adsorption and $1/n$ is related to the adsorption intensity, which varies with heterogeneity of the material. The values of $1/n$ lying between 0 and 1 and the n values lying in between 1 and 10 indicated that the conditions are favorable for adsorption. The values of K_f and $1/n$ calculated from the intercept and slope of the plot of $\ln q_e$ vs. $\ln C_e$ at different temperatures shown in Fig. 10 are listed in Table 1. For these adsorption processes, n values have been found to vary between 1.27 and 1.46, therefore, fluoride adsorption on PCP at different temperature represents beneficial adsorption. The high correlation coefficient (R^2) >0.99 indicates that the Freundlich isotherm fitted well with the experimental data.

By the analysis of the above two isotherms, it comes to a conclusion that fluoride adsorption on PCP follows both Freundlich and Langmuir isotherms, indicating both monolayer and heterogeneous surface conditions may exist. By the analysis of the above two isotherms, it comes to a conclusion that fluoride adsorption on PCP follows both Freundlich and Langmuir isotherms. The results revealed that the adsorption process was a combined process of homogeneous and heterogeneous adsorption, while the effects of indirect adsorbate and adsorbent interactions on adsorption process could be neglected. Thus the adsorption occurred mainly via the electrostatic interactions between fluoride and positively charged amino groups as well as physical forces. Besides, compared to the results mentioned in the research [13], PCP has a slightly higher adsorption capacity than PCB (protonated chitosan beads), which may be attributed to the bigger specific surface area relative to PCB.

3.8. Sorption mechanism

Accord to the FTIR spectra of the fluoride treated PCP mentioned in Section 3.1, it was not difficult to find that the peak of $-\text{NH}_3^+$ at 1516 cm^{-1} almost disappear, which results from the strong electrostatic attraction between positive charged $-\text{NH}_3^+$ and negatively charged fluoride ions. Hence, the above observation shows that the adsorption process of fluoride on PCP might be achieved through electrostatic attraction between positively charged surface and negatively charged fluoride ions. Moreover, PCP may be considered as hard acid due to many H^+ ions and hence would prefer to bind with hard base (fluoride ion), which may be another driving force for fluoride adsorption.

3.9. Desorption and regeneration

Any adsorbent is economically viable if the adsorbent can be regenerated and reused. The exhausted PCP were regenerated using HCl, H_2SO_4 and NaOH solutions. All the regeneration experiments were carried out at room temperature. The results (Fig. 11) show that HCl is a better eluent compared with H_2SO_4 and NaOH. After the exhausted PCP were regenerated with 0.1 M HCl solution, this adsorbent still allows a high removal toward fluoride.

Table 1
Langmuir and Freundlich isotherm parameters of fluoride adsorption onto PCP.

Isotherms	Parameters	293 K	303 K	313 K	323 K
Langmuir isotherm	Q	8.10	9.25	9.71	10.52
	b	0.089	0.052	0.039	0.032
	R_L	0.160–0.488	0.245–0.618	0.306–0.682	0.346–0.726
	R^2	0.990	0.974	0.987	0.977
Freundlich isotherm	K_f	0.784	0.570	0.456	0.413
	$1/n$	0.683	0.733	0.765	0.785
	n	1.46	1.37	1.31	1.27
	R^2	0.996	0.999	0.998	0.999

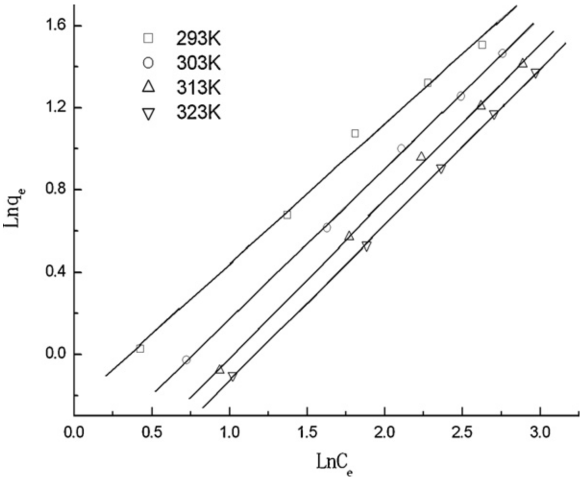

Fig. 10. Freundlich isotherm plots for fluoride adsorption on PCP.

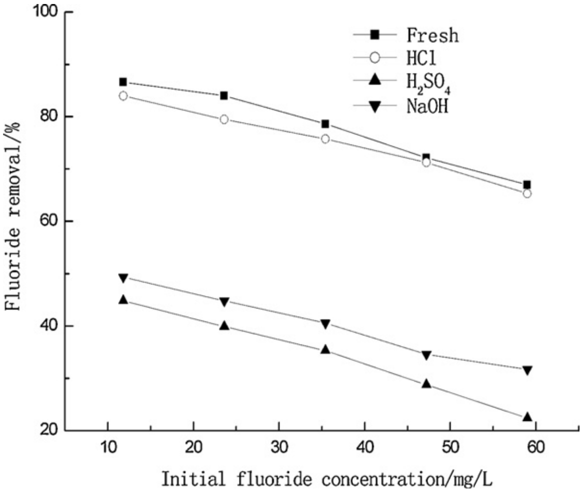

Fig. 11. Regeneration of PCP.

4. Conclusions

Through cross-linked and protonated modifications, chitosan was used for fluoride removal from aqueous solution. Batch experiments were conducted to investigate the adsorption capacity and the regeneration feasibility of this adsorbent. XRD and FTIR analysis showed that the modified chitosan with lower crystal energy and protonated amino groups were favorable for fluoride adsorption. Also, SEM analysis suggested the occurrence of fluoride adsorption onto PCP. pH 7.0 was chosen as the optimal value. The equilibrium data fitted well with Langmuir and Freundlich isotherm models, and the maximum monolayer adsorption capacity was 8.10 mg g^{-1}at room temperature. In addition, the constant values of R_L and $1/n$ indicated that fluoride adsorption was favorable. The presence of coexisting anions weakened fluoride adsorption, especially the high valence anion such as sulfate. This adsorbent was regenerated with HCl effectively and had good performance for repeated use. Electrostatic attraction was the main driving forces for fluoride adsorption.

Acknowledgments

Financial support by the National Natural Science Foundation of China Project (Grant No. 51003086) and National Higher Education Institution General Research and Development Project are gratefully acknowledged.

References

[1] Y. Wang, E.J. Reardon, Applied Geochemistry 16 (2001) 531–539.
[2] H. Lounici, L. Addour, D. Belhocine, H. Grib, S. Nicolas, B. Bariou, N. Mameri, Desalination 114 (1997) 241–251.
[3] M. Srimurali, A. Pragathi, J. Karthikeyan, Environmental Pollution 99 (1998) 285–289.
[4] M. Hichour, F. Persin, J. Sandeaux, C. Gavach, Separation and Purification Technology 18 (2000) 1–11;
WHO, Guidelines for Drinking Water Quality, Geneva, 2004.
[5] N. Parthasarathy, J. Buffle, W. Haerdi, Canadian Journal of Chemistry 64 (1986) 24–29.
[6] I.B. Solangi, S. Memon, M.I. Bhanger, Journal of Hazardous Materials 171 (2009) 815–819.
[7] S. Meenakshi, N. Viswanathan, Journal of Colloid and Interface Science 308 (2007) 438–450.
[8] N. Viswanathan, S. Meenakshi, Journal of Hazardous Materials 162 (2009) 920–930.
[9] P. Sehn, Desalination 223 (2008) 73–84.
[10] S.K. Adhikary, U.K. Tipnis, W.P. Harkare, K.P. Govindan, Desalination 71 (1989) 301–312.
[11] M. Mohapatra, S. Anand, B.K. Mishra, D.E. Giles, P. Singh, Journal of Environment Management 91 (2009) 67–77.
[12] P. Miretzky, A.F. Cirelli, Journal of Fluorine Chemistry 132 (2011) 231–240.
[13] N. Viswanathan, C. Sairam Sundaram, S. Meenakshi, Journal of Hazardous Materials 161 (2009) 423–430.
[14] N. Viswanathan, C.S. Sundaram, S. Meenakshia, Colloids and Surfaces B: Biointerfaces 68 (2009) 48–54.
[15] A. Bansiwal, D. Thakre, N. Labhshetwara, S. Meshram, S. Rayalu, Colloids and Surfaces B: Biointerfaces 74 (2009) 216–224.
[16] N. Li, R. Bai, Industrial and Engineering Chemistry Research 44 (2005) 6692–6700.
[17] S. Jagtap, D. Thakre, S. Wanjari, S. Kamble, N. Labhsetwar, S. Rayalu, Journal of Colloid and Interface Science 332 (2009) 280–290.
[18] I. Langmuir, Journal of the American Chemical Society 38 (1916) 2221–2295.
[19] H.M.F. Freundlich, Zeitschrift fur Physikalische Chemie 57A (1906) 385–470.
[20] K.R. Hall, L.C. Eagleton, A. Acrivos, T. Vermeulen, Industrial and Engineering Chemistry Fundamentals 5 (1966) 212–219.